Mechanical compaction of porous sandstone: an experimental study using acoustic emission (AE) monitoring.

AE monitoring during compaction of sandstone

J. Fortin*, S. Stanchits, G. Dresen**, Y. Guéguen***

**Laboratoire de Géologie*
Ecole Normale Supérieure
24 Rue lhomond
75005 Paris – France
fortin@geologie.ens.fr

***GeoForshungsZentrum Potsdam*
Haus D – Pojekbereich 3.2
Telegrafenberg
D-14473 Potsdam – Germany
stanch@gfz-potsdam.de

ABSTRACT. *In some reservoirs, large deformations occur during oil or gas production because of the effective stress change. For very porous rocks, these production operations can be sufficient to cause inelastic deformation and irreversible damage. Rock formations can undergo deformation by different mechanisms, including dilatancy or pore collapse. In the laboratory, the spatial evolution of damage as well as the source mechanism can be followed using the acoustic emissions. In this paper, we present three different laboratory axisymmetric compression experiments. Indeed, when subjected to an overall compressive loading, a porous rock may fail by shear localisation, compaction localization, or by cataclastic flow.*

KEY WORDS: Porous rock, acoustic emissions locations, shear localization, compaction bands, cataclastic flow.

1. Introduction

Compaction of porous rock is an important process in the oil and gas industry. Compaction caused by changes in effective stresses during production can, lead to seafloor subsidence (for example, the extraction of oil and gas in the Ekofisk field in the North Sea has produced a subsidence of more than 4 meters), cause casing failures, or can decrease significantly the permeability of the reservoir.

Three different deformation modes can be observed in porous sandstone (Wong et al. 1997, Klein et al. 2001, Fortin et al. 2005): when subjected to an overall compressive loading, a rock can fail by shear localization, compaction localization or cataclastic flow. Cataclastic flow is commonly observed in a response to purely hydrostatic loading: at a critical pressure grains are crushed and the pore collapse, resulting in a large decrease in porosity (Zhang et al. 1990). A deviatoric stress field can lead to localized deformation. Under low mean pressure, localization in porous rock is associated with the formation of shear bands (e.g. Wong et al 1997). However under certain conditions, localization can occur purely by compaction, without evident shear (formation of compaction bands) (e.g. Klein et al. 2001, Rudnicki 2004).

Although the three modes of failure are very different on the macroscopic scale, they involve the same micromechanical processes. Indeed, grain-scale microcracking is commonly observed and leads to radiation of acoustic emissions. Different authors have used the acoustic emissions technique in axisymmetric compression experiments to investigate shear fracture nucleation (e.g Lei 1992, Lockner 1993). Recently, Fortin et al. (2006) have used 3D locations of acoustic emission to analyse the development of compaction bands.

In this paper, we report the acoustic emission location recorded during three axisymmetric compression experiments performed on Bleurswiller sandstone. The first is a purely hydrostatic one. The second and the third one are triaxial compression tests at effective confining pressures of 10 MPa and 70 MPa. Shear localization is observed in the second test, whereas compaction localization is observed in the third one. In addition the source mechanisms have been investigated in order to compare these three modes of deformation.

2. Materials and Methods

2.1. Sample

Cylindrical specimens of 100 mm in length and 50 mm in diameter were prepared from Bleurswiller sandstone. Figure 1a) gives a picture of an intact specimen. Porosity is about 25 %. Fortin et al., (2006) have investigated microstructure using optical microscopy: this gray sandstone contains ~50 % quartz, ~30% feldspars, and ~20 % oxydes-micas. Grain sizes range from 80 μm to 150 μm with a mean value of 110 μm. Figure 1b) show a SEM (scanning electron

microscopy) of an intact specimen, for comparison: porosity appears in black and quartz grains appear darker than the feldspar grains.

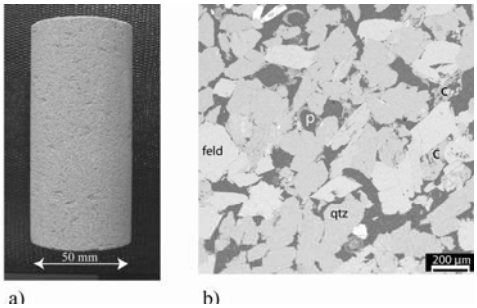

Figure 1. *a) Picture of a non-deformed sample of Bleurswiller sandstone. b) SEM micrograph (backscattered) of intact sandstone. Epoxy-filled pores (p) appear in black, porosity is about 25%. Quartz, feldspar, and clay are denoted by qtz, feld, and c, respectively.*

2.2. Mechanical Data

The experiments were performed at the GeoForschungsZentrum Potsdam. We used a servo controlled loading frame from MTS Systems Corporation (Figure 2a). All experiments were carried out at room temperature. The two triaxial experiments were carried out at a constant strain rate of $10^{-5}s^{-1}$. The samples were saturated with distilled water and deformed under fully drained conditions at a constant pore pressure of 10 MPa. The pore pressure was maintained constant, and the variation of pore volume was recorded using a volumometer. From this, the evolution of connected sample porosity was deduced.

2.3. Acoustic Emission Monitoring

AE activity and velocity changes were monitored by twelve *P*-wave piezoelectric sensors either embedded in the pistons or glued to the sample surface and sealed in a Neoprene jacket using two-component epoxy (Figure 2b). *P*-wave sensors were produced from PZT piezoceramic plates 5 mm diameter and 2 mm thickness. Transducer signals were amplified by 40 dB using Physical Acoustic Corporation preamplifiers. Full-waveform AE data and the ultrasonic signals for P-wave velocity measurements were stored in a 12 channel transient recording system (*DaxBox*, *Prökel*, Germany) with an amplitude resolution of 16 bit at 10 MHz sampling rate. For periodic elastic wave speed measurements, six *P*-sensors were used as senders applying 100V pulses every ~30 seconds during loading.

Ultrasonic transmissions and AE waveforms were discriminated automatically after the experiments. Advance software was used to automatically pick up onset time of *P*-wave and AE. Hypocenter locations were estimated using a downhill simplex algorithm considering time-dependent changes of the anisotropic velocity field. AE hypocenter location errors are estimated to be ~2.5 mm. First motion amplitudes were picked automatically and first motion polarities were used to

discriminate AE sources types in tensile, shear, and collapse events (Zang et al, 1998).

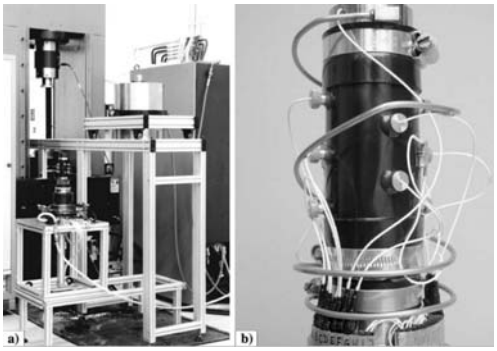

Figure 2. *Experimental setup. a) MTS loading frame with 200 MPa pressure vessel. b) Cylindrical specimen encapsulated in rubber jacket with P-sensors glued directly on the sample surface.*

3. Results and discussion

3.1. Mechanical data

In this paper, we use the convention that compressive stresses and compactive strains are positive. The maximum and minimum (compressive) stresses are denoted by σ_1 and σ_3. The pore pressure is denoted by P_p, and the difference between the confining pressure ($P_c = \sigma_1 = \sigma_2$) and the pore pressure is referred to as the "effective confining pressure". The effective mean stress $(\sigma_1+2\sigma_3)/3 - P_p$ will be denoted *P* and the differential stress $\sigma_1-\sigma_3$ by *Q*.

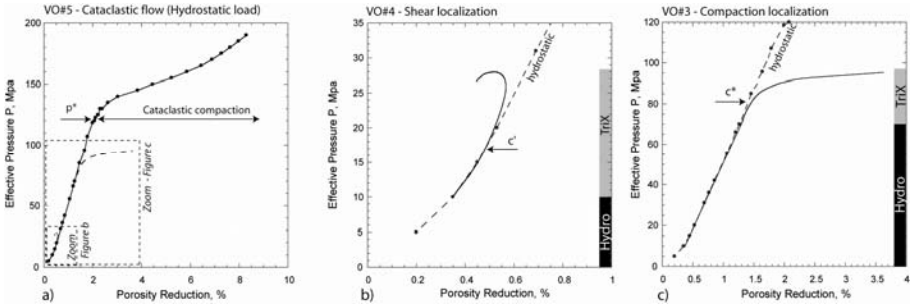

Figure 3. *Effective mean pressure versus porosity reduction. a) Hydrostatic loading (for reference, the two triaxial experiments are shown as the dashed lines). b) and c) Triaxial compression experiments performed at effective confining pressure of 10 MPa and 70MPa, respectively (for reference, the hydrostatic loading is shown as the dashed line). The critical stress state P*, C' and C* are indicated by arrows.*

Figure 3a) illustrates the hydrostatic compaction behaviour. In the first part of the loading, the pore space is initially tightened by elastic deformation. However at

the stress state P*, the sample shows a dramatic reduction in porosity reduction (cataclastic flow). This inflection point P* occurs at an effective pressure of ~120 MPa. This critical stress state is associated with the onset of grain crushing (Zhang et al. 1990). The grains are crushed and the pores collapse, resulting in an overall decrease in porosity.

The sample deformed at an effective confining pressure of 10 MPa is representative of the brittle faulting regime (Figure 3b and 4b). The differential stress attained a peak, beyond which strain softening was observed (Figure 4b). The porosity initially decreased, but a stress state C' it reversed to an increase indicating dilatation of the pore space (Figure 3b).

In contrast, for the sample deformed at an effective confining pressure of 70 MPa, the failure mode is associated with an appreciable porosity reduction (Figure 3c). In the first part of the loading, the triaxial data (solid curve) coincides with the hydrostat (dashed curve). However at stress state higher than C* the deviatioric stress field provided significant contribution to the compactive strain (Figure 3c). During this second stage strain hardening is observed (Figure 4c).

In these three experiments 'inelastic' compaction is characterized by marked enhancement of acoustic emission (AE) activity (dashed lines in Figure 4).

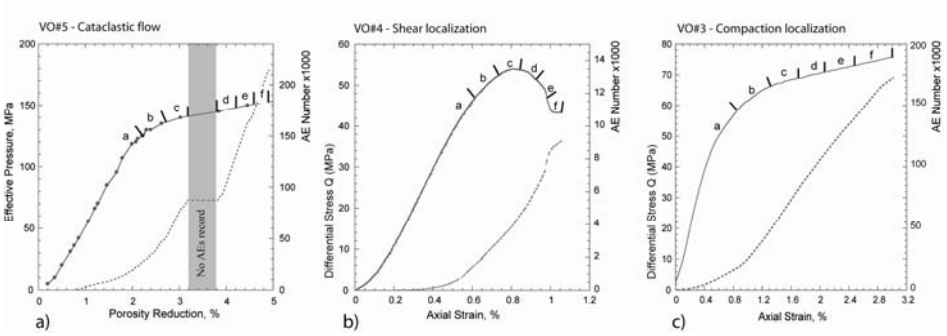

Figure 4. *a) Hydrostatic experiment: Effective pressure (solid curve) and cumulative AE (dotted line) as functions of porosity reduction. b) and c) Triaxial experiments : differential stress (solid curve) and accumulative AE (dotted line) versus axial. Effective confining pressure was 10 MPa in Figure b) and 70 MPa in Figure c). Six intervals are defined for each experiment (a to f) corresponding to the AE hypocenter distributions shown in Figure 5.*

3.3 Locations of the AE hypocenters

Cataclastic flow. AE locations from sample deformed under a hydrostatic loading are shown in Figure 5– Top and can be compared to the stress-strain curve plotted in Figure 4a. For an idealized sandstone made as a randomly packed assemblage of spherical particles of several distinct sizes, the critical pressure P* can be modelled as the result of stress concentration at the grain contacts, making the rock susceptible to grain crushing and grain rearrangement (Zhang et al. 1990). However our AE locations show that this process is not homogeneous. In stages a to c, AE events form clusters. The clusters coalesce and form compacted zones randomly oriented.

In stages e and f, the compaction seems to be more homogeneous. Material heterogeneities and in particular high porosity regions may influence the nucleation process.

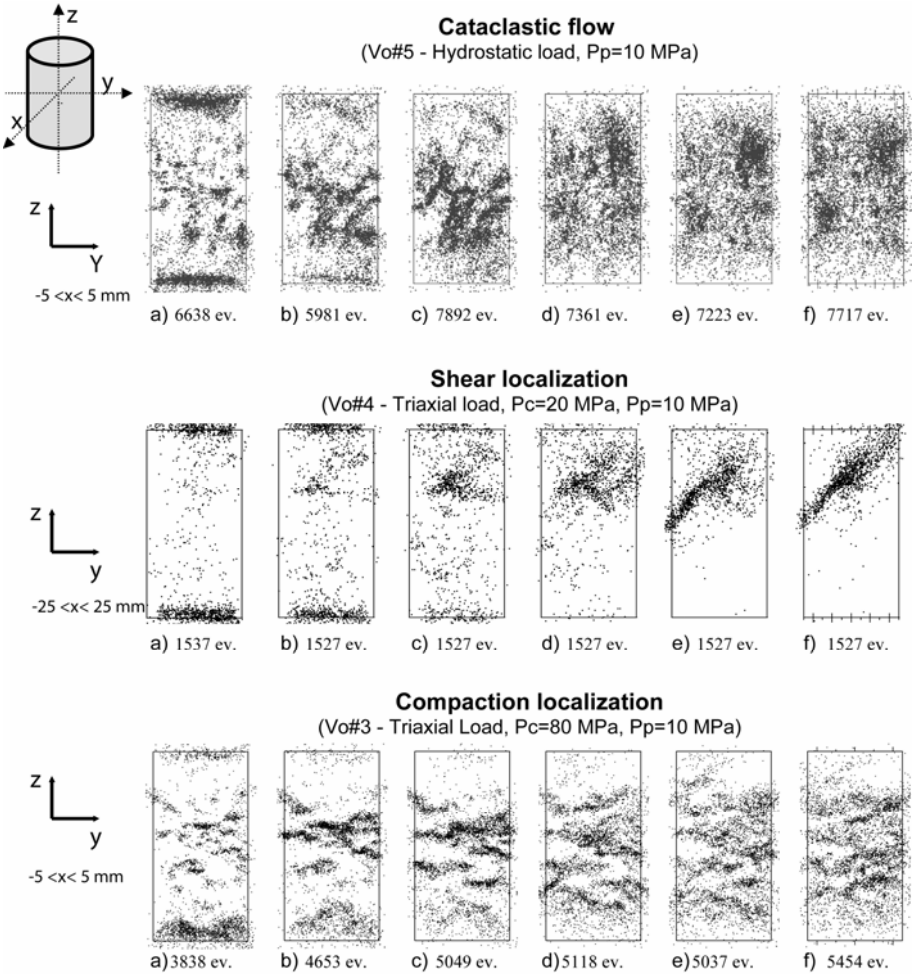

Figure 5. *AE hypocenter distribution. The intervals (a to f) are defined in Figure 4. Top plot is a projection of all the events located between -5mm<x<5mm, on the (z,y) plane recorded during the hydrostatic experiment. Middle plot is a projection of all the events on the (z,y) plane recorded during the triaxial experiment at 10 MPa effective confining pressure. Bottom plot is a projection of all the all the events located between -5mm<x<5mm, on the (z,y) plane recorded during the triaxial experiment at 70 MPa effective confining pressure.*

Shear localization. AE locations from sample deformed in the brittle regime are shown in Figure 5-Middle and can be compared to the stress-strain curve plotted in

Figure 4b. In stage a), AE activity occurred -beginning with the initial loading- at the ends of sample, may be due to end cap friction. Stage b shows diffusely spaced AE events in the pre-nucleation stage. Next, the fault nucleates rapidly (stages d-e) with the fault orientation clearly observable.

Compaction localization. A number of features of this experiment (Figures 5-bottom and 4c) differs from the behaviour of the rock in the brittle regime. In stages a to f, AE events form clusters that are elongated mostly normal to the compression direction, and form several discrete compactions bands. The overall AE activity is also more intense: 13 times more events were recorded during compaction localization than during shear localization. We interpret the enhanced AE activity as 1) the result of grain crushing and 2) the fact that this kind of experiment allows the formation of several localizations.

3.4 AE Focal mechanisms

During the experiments, the full-waveform AE data are recorded which allows us to conduct *P* wave first-motion studies (see Lei et al. 1992 and Stanchits et al. 2001). In our experiment local AE source mechanism were separated into pure tensile mechanism (T), shear type events (S) and implosion type events (C) representing tensile cracks, shear cracks and pore collapse, respectively.

In the three experiments (Figure 6), the source type distribution reveals a dominance of pore collapse (C-type). The distribution is almost the same during compaction localization and cataclastic flow (Figure a and c), indicating that the micro-mechanisms are similar. However, the development of a shear band (Figure b) is associated with an increase of the shear type events: at the end of this experiment, ~55% of the events represent shear cracks.

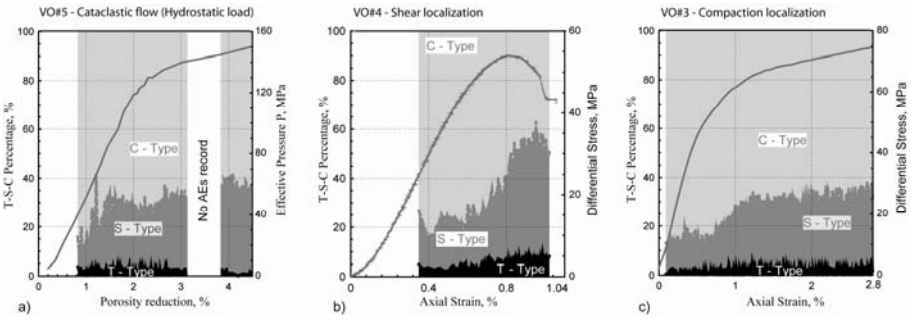

Figure 6. *Color code indicates AE-source type distribution during loading. C-, S-, and T-types events possibly represent signals radiated from pore collapse, shear and tensile cracks, respectively. The percentages of each part are indicated on the left vertical sale in the three plots: for example in Figure a) T-type, S-type, and C-type represent, respectively, ~5%, ~27% and ~67% of the source mechanism. For reference, the evolution of effective pressure (right vertical scale) is plotted versus porosity reduction in Figure a). The evolution of differential stress versus axial strain (right vertical scale) is plotted in Figure b) and c).*

4. Conclusions

In this paper, three modes of deformation were investigated during the compaction of porous rock. Under hydrostatic pressure, a large mechanical decrease of porosity is observed at a critical pressure, where pore collapse and grain crushing occur. Under axisymmetric compression, the mechanical response of the sample deformed at 10 MPa effective confining pressure is characterized by brittle faulting. However at 70 MPa effective confining pressure, compaction bands can be observed. Acoustic Emission record provides important information to understand these three modes of deformation: 1) the occurrence of AE activity is associated with the development of inelastic strain; 2) AE locations allows us to characterize the spatial evolution of the damage in the rock; 3) finally first-motion studies, which give an estimation of the source mechanisms taking place in the sample, allowing us to better understand the micro-mechanisms.

5. Bibliography/References

Fortin, J., Stanchits, S., Dresen G., and Guéguen Y., "Acoustic emission and velocities associated with the formation of compaction bands", *J. Geophys. Res.*, 111, 2006, B10203, doi:10.1029/2005JB003854.

Fortin, J., Schubnel A., and Guéguen Y., "Elastic wave velocities and permeability evolution during compaction of Bleurswiller sandstone", *Int. J. Rock. Mech. Min. Sci Geomech.*, 42, 2005, 873– 889.

Klein, E., Baud P., Reuschle T., and Wong T.-F., "Mechanical behaviour and failure mode of Bentheim sandstone under triaxial compression", *Phys. Chem. Earth*, Part A, 26, 2001, 21– 25.

Lei, X, Nishizawa O., Kose K. and Satoh T., "Fractal structure of the hypocenter distributions and focal mechanism solutions of acoustic emission in two granites of different grain sizes". J. Phys. Earth., 40, 1992, 617-634.

Lockner, D. A., "The role of acoustic emission in the study of rock fracture", *Int. J. Rock Mech. Min. Sci. Geomech.*, 30, 1993, 883– 899.

Rudnicki, J. W., "Shear and compaction band formation on an elliptic yield cap", *J. Geophys. Res.*, 109, 2004, B03402, doi:10.1029/2003JB002633.

Stanchits, S., Zang A., and Dresen G., "Focal mechanisms of acoustic emission events during fault propagation and friction sliding", Eos Trans. AGU, 82(47), 2001, Fall Meet. Suppl., Abstract T51A-0847.

Wong, T.-F., David C., and Zhu W., "The transition from brittle faulting to cataclastic flow in porous sandstone: Mechanical deformation", *J. Geophys. Res.*, 102, 1997, 3009–3025.

Zang, A., Wagner, F.C, Stanchits, S., Janssen, C. and Dresen G. "Fracture process zone in granite", *J. Geophys. Res.*, 105, 1998, 651–661.

Zhang, J., Wong T.-F, and Davis D.M. "Micromechanics of pressure-induced grain crushing in porous rocks", *J. Geophys. Res.*, 95, 1990, 341–352.